analytical chemistry

Technical Note

Cite This: *Anal. Chem.* 2019, 91, 4975−4979

pubs.acs.org/ac

Protein Characterization in 3D: Size, Folding, and Functional Assessment in a Unified Approach

Morten E. Pedersen,[†] Sarah I. Gad,[†] Jesper Østergaard,[†,‡] and Henrik Jensen*[,†,‡]

[†]FIDA-Tech ApS, Universitetsparken 2 (C/O University of Copenhagen), 2100 Copenhagen, Denmark

[‡]Department of Pharmacy, University of Copenhagen, Universitetsparken 2, 2100 Copenhagen, Denmark

Supporting Information

ABSTRACT: Assessment of protein stability and function is key to the understanding of biological systems and plays an important role in the development of protein-based drugs. In this work, we introduce an integrated approach based on Taylor dispersion analysis (TDA), flow induced dispersion analysis (FIDA), and in-line intrinsic fluorescence which enables rapid and detailed assessment of protein stability and unfolding. We demonstrate that the new platform is able to efficiently characterize chemically induced protein unfolding of human serum albumin (HSA) in great detail. The combined platform enables local structural changes to be probed by monitoring changes in intrinsic fluorescence and loss of binding of a low-molecular weight ligand. Simultaneously, the size of the unfolding HSA is obtained by TDA on the same samples. The integration of the methodologies enables a fully automated characterization of HSA using only a few hundred nanoliters of sample. We envision that the presented methodology will find applications in fundamental biophysics and biology as well as in stability screens of protein-based drug candidates.

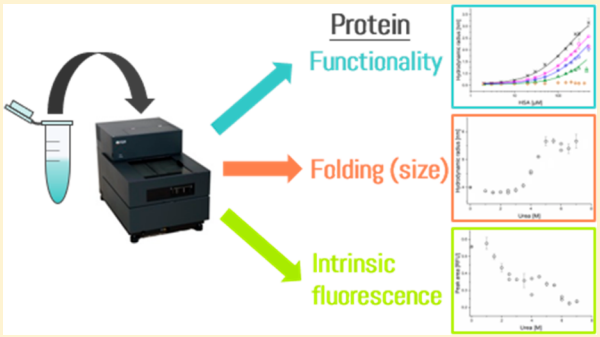

Protein stability and function is currently assessed using an array of different methodologies such as dynamic light scattering (DLS), small angle X-ray scattering (SAXS), size exclusion chromatography (SEC), SDS-page, and spectroscopic methods, including UV absorption, fluorescence, circular dichroism (CD), and IR spectrometry, in order to give a full detailed picture.[1−4] However, often limitations are encountered as some techniques require large amounts of sample, have a low throughput, and/or require highly purified proteins.

In this work we present a unified flow based approach based on Taylor dispersion analysis (TDA),[5−10] flow induced dispersion analysis (FIDA),[11−13] and intrinsic fluorescence. TDA and FIDA have the advantage of low sample volume requirements (nanoliters) and possibility of automation; however, they have until now mainly been used for size-based characterization and assessment of noncovalent interactions, respectively.

Here, we combine for the first time TDA and FIDA with UV-fluorescence in order to realize a platform for detailed automated protein characterization. The urea-induced human serum albumin (HSA) unfolding was observed as a change in apparent size of HSA as well as by local structural changes close to the tryptophan and tyrosine residues as measured by fluorescence emission. The loss of binding of the HSA ligand fluorescein (a small molecular probe binding to Sudlow site 1 (domain IIA) in HSA),[14] as measured by FIDA, was observed during the unfolding process. Interestingly, the three approaches detected the different phenomena occurring in the chemically induced denaturation of HSA: (1) loss of function as measured by a lower binding affinity of the ligand fluorescein, (2) structural changes around the tyrosine and tryptophan residues as measured by a decrease in intrinsic fluorescence, and (3) global protein unfolding as measured by a change in size (hydrodynamic radius). The three approaches provide different information, the combination of which gives a detailed description of the HSA denaturation and unfolding process. The approach may easily be transferred to other proteins and may be of particular interest when limited sample availability, sensitivity, or matrix interferences prevent the use of other methods.

EXPERIMENTAL SECTION

Equipment. The FIDA and TDA experiments were conducted on a capillary electrophoresis instrument (PrinCE NEXT 870, PrinCE Technologies, Emmen, The Netherlands). The FIDA experiments employed laser-induced fluorescence (LIF) detection (ZETALIF Evolution, Picometrics) with excitation wavelength 488 nm (Melles Griot Diode laser, Picometrics, Labege, France), while the TDA experiments utilized intrinsic LIF detection with excitation wavelength 266 nm (SNU-02P-100 laser, Teem Photonic, Meylan, France),

Received: January 30, 2019
Accepted: March 27, 2019
Published: March 27, 2019

DOI: 10.1021/acs.analchem.9b00537
Anal. Chem. 2019, 91, 4975−4979

both setups utilized a high-pass filter. A standard fused silica capillary (inner diameter 75 μm, outer diameter 375 μm, total length 100 cm, length to detection window 90 cm) purchased from Polymicro Technologies (Phoenix, Arizona, USA) was used. The capillary was temperature-controlled to 25 °C inside the PrinCE instrument, except for the minor part connected to the external detector. Capillary inlet and samples were also temperature-controlled to 25 °C.

Materials and Chemicals. Ultrapure water (18.2 MΩ-cm at 25 °C) was obtained from a SG Ultraclear water purification system (SG Water, Barsbüttel, Germany). Human serum albumin (HSA, fatty acid free), fluorescein, urea, and acetone were purchased from Sigma-Aldrich (St Louis, Missouri, USA). Sodium hydrogen phosphate monohydrate, disodium hydrogen phosphate dodecahydrate, and sodium hydroxide were purchased from Merck (Darmstadt, Germany).

All prepared solutions were filtered through a Q-max 0.45 μm nylon syringe filter (Frisenette, Knebel, Denmark).

A 67 mM phosphate buffer, pH 7.4, was prepared using ultrapure water and used as working buffer.

Unfolding of HSA. Stock solutions of 120 μM HSA and 10 M urea was prepared in 67 mM phosphate buffer, pH 7.4. Subsequently, HSA was diluted to a fixed concentration of 15 μM in varying concentrations (0−7 M) of urea. All samples were preincubated for >10 min to reach equilibrium prior to analysis.

Fluorescein Binding to HSA at Varying Urea Concentrations. A stock solution of 1 mM fluorescein was prepared in acetone and then diluted to a fixed indicator concentration of 10 nM in varying analyte concentrations of HSA (0−500 μM) and urea (0−4 M). A stock solution of 750 μM HSA was prepared in the phosphate buffer, and diluted into the following analyte concentration ranges: 0−500 μM in 0, 1, and 2 M urea, 0−450 μM in 3 M urea, and 0−400 μM in 4 M urea. All samples were preincubated for >10 min to reach equilibrium prior to analysis.

Procedures. The capillary based methods are illustrated in Figure 1.

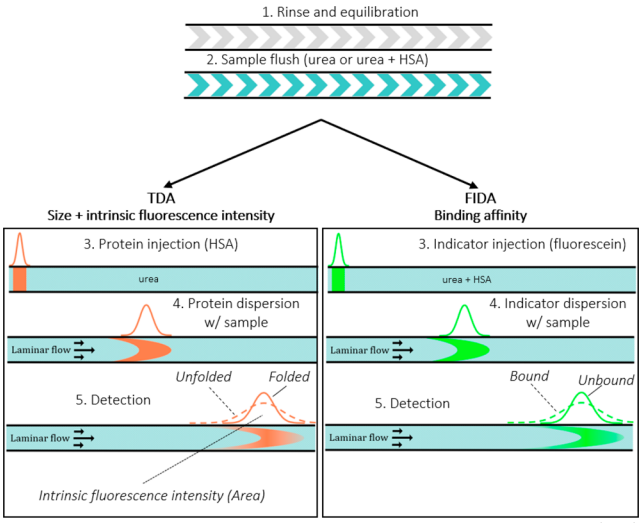

Figure 1. Schematics showing the automated workflow for TDA (left) and FIDA (right). TDA probes protein size and intrinsic fluorescence intensity, while FIDA measures binding affinity and apparent size of the indicator−analyte complex.

The TDA and FIDA experiments were conducted using the following method. The capillary was rinsed prior to sample analysis with 1 M NaOH followed by 67 mM phosphate buffer at 1500 mbar for 3 min each. The analyte sample was injected applying 1500 mbar for 60 s, subsequently the indicator sample was injected applying 100 mbar for 5 s (corresponding to filling 1% of the capillary volume) followed by a dipping step into pure phosphate buffer. The injected indicator sample was then mobilized toward the detector with the analyte sample applying a pressure of 400 mbar for maximum 330 s. All samples were analyzed in triplicate unless otherwise noted.

The capillary outlet was submersed into ultrapure water to avoid buildup of urea residues on the capillary outlet and subsequent clogging.

Data Analysis. The Taylorgrams were processed using FIDA Data Analysis Software, version 01 (FIDA-Tech ApS, Copenhagen, Denmark) in order to calculate the hydrodynamic radius. Evaluation of the fulfillment of the Taylor's conditions was performed applying the FIDA Assay Development Tool PRO (FIDA-Tech ApS). The equations utilized by the software can be found in the Supporting Information.

The apparent diffusivity of the indicator may be treated as a weighted average of the diffusivities of the bound and unbound indicator.[11] Assuming a low concentration of the indicator relative to the protein, a one-to-one binding stoichiometry and that the system is at equilibrium the binding isotherm may be described by[12]

$$D_{app} = \frac{D_I - D_{IA}}{[A]K_d^{-1} + 1} + D_{IA} \quad (1)$$

where K_d is the dissociation constant, [A] is the formal analyte concentration, and D_{app}, D_I, and D_{IA} are the apparent, indicator, and complex diffusivity, respectively. The diffusivities may be converted to hydrodynamic radii using the Stokes−Einstein equation:

$$R_{app} = \frac{k_B T}{6\pi\eta D_{app}} \quad (2)$$

where R_{app} is the apparent hydrodynamic radius, T is the absolute temperature, and k_B is Boltzmann's constant.

Combination of eqs 1 and 2 results in the following binding isotherm (3):

$$R_{app} = \frac{1 + \frac{1}{K_d}[A]}{((R_I)^{-1} - (R_{IA})^{-1}) + \left(1 + \frac{1}{K_d}[A]\right)(R_{IA})^{-1}} \quad (3)$$

where R_I and R_{IA} are the indicator and complex hydrodynamic radius, respectively.

The viscosity of the sample introduced into the capillary was calculated from the expression

$$\eta_{sample} = \frac{t_{R_{sample}}}{t_{R_{reference}}} \cdot \eta_{reference} \quad (4)$$

where the reference viscosity was set to 0.890 mPa·s at 25 °C based on the assumption that the sample without urea (i.e., 67 mM phosphate buffer) was similar to the viscosity of water.[15] The sample viscosity was subsequently used for calculating the viscosity-compensated hydrodynamic radius.

DOI: 10.1021/acs.analchem.9b00537
Anal. Chem. 2019, 91, 4975−4979

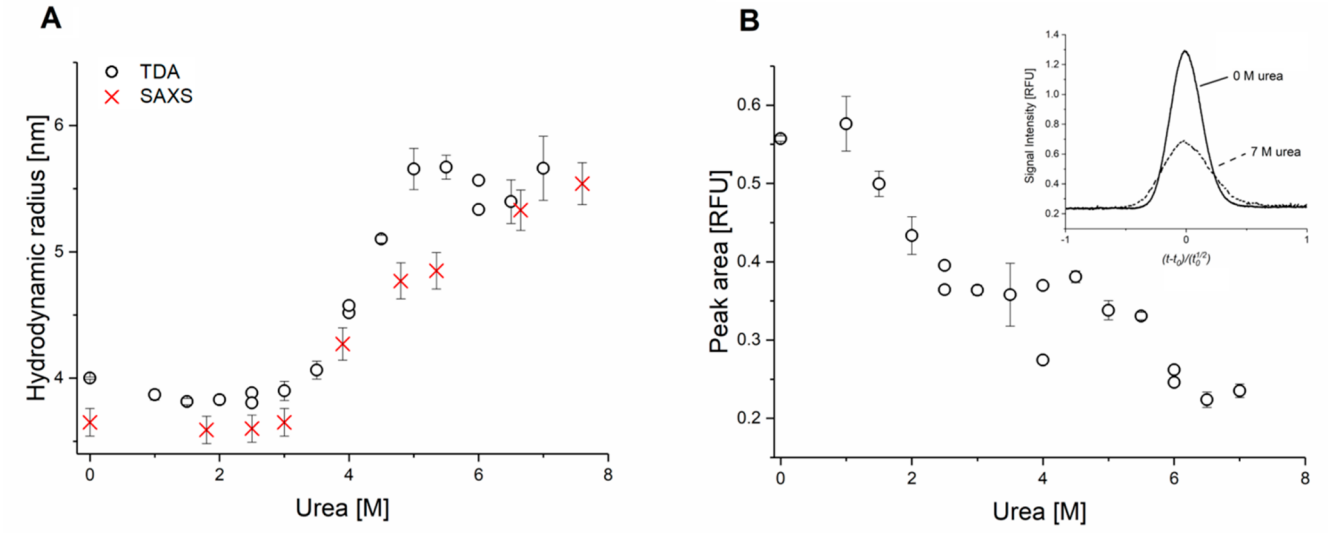

Figure 2. (A) Hydrodynamic radius of HSA as a function of urea concentration determined by TDA (15 μM HSA; open circles) at 25 °C compared to SAXS (15−45 μM HSA; red crosses, data of Leggio et al.[17]) at 25 °C. (B) Intrinsic fluorescence area of 15 μM HSA as a function of urea concentration corrected for response factor (see the Supporting Information). (insert) Overlay of Taylorgrams at 0 and 7 M urea (solid and dashed line, respectively), corrected for viscosity changes according to Chamieh et al.[19] TDA measurements were performed in triplicate, excluding urea concentrations 2.5, 4, and 6 M, which were duplicates.

RESULTS AND DISCUSSION

The current tools for measuring chemically induced unfolding of proteins may be grouped as global and local.[16] Global methodologies such as DLS and SAXS provide insights into changes in the overall protein size but do not provide specific information on which regions are affected during unfolding and denaturation. Local changes may be probed by monitoring local optical properties such as intrinsic fluorescence, CD, or changes in binding affinity at specific sites in proteins,[17,18] but they are not necessarily a good measure of global unfolding of the protein. Typically, a detailed picture of the unfolding process can therefore only be reached by combining several techniques which may be challenging due to scarcity of material.

Albumin is an abundant serum protein that serves as transporter of small molecules such a fatty acids, amino acids, and low-molecular weight drug compounds.[20] Albumin is composed of three domains (I, II, and III) each having additional subdomains. The unfolding of HSA has previously been studied using different techniques, which has provided indications of a sequential unfolding process.[17,21] HSA exhibits a relatively complicated unfolding pattern and may therefore be used to assess the potential of analytical methodologies for studying unfolding and stability of multidomain proteins, molecular constructs and complexes. In this work, global changes are addressed using TDA for measuring the overall hydrodynamic radius, and HSA intrinsic fluorescence intensity is utilized for addressing local structural changes associated with the tyrosine and tryptophan residues. The low-molecular weight ligand fluorescein has been reported to bind to domain IIA (Sudlow site I)[14] and may therefore be used to probe structural changes in this specific part of HSA. It should be noted that the unfolding process was studies under equilibrium conditions. The present set of experiments does not provide kinetic information on the protein folding process.

Urea-Induced Unfolding of HSA as Measured by Taylor Dispersion Analysis. The hydrodynamic radius of HSA was measured by TDA as a function of urea concentration (Figure 2A), at 0 M urea it was determined to 4.0 nm which were in line with previous TDA measurements of native HSA.[22] The hydrodynamic radius of HSA increased gradually from 4.0 to 5.7 nm as induced by increasing urea concentration (0−7 M). The global HSA unfolding started at 4.0 M urea and subsequently plateaued at 5−7 M urea. The obtained results correlated well with a similar study utilizing urea-induced unfolding of HSA monitored with small-angle X-ray scattering (SAXS);[17] see Figure 2A.

Furthermore, the peak areas of the Taylorgrams were exploited for simultaneously probing the intrinsic fluorescence intensity of HSA at increasing urea concentration (Figure 2B). Interestingly, the intrinsic fluorescence of HSA was affected by the presence of urea already at 1.5 M as seen by a decline from the plateau at 0−1 M urea, whereas a notable change in the hydrodynamic radius of HSA was not detected below 4 M urea. Apparently, HSA was undergoing structurally local changes prior to the overall unfolding. Furthermore, it can be located to the proximity of the tryptophan and tyrosine residues, since the intrinsic fluorescence is affected upon exposure to the solvent.

The observed pattern in Figure 2B, with two plateaus at 0−1 M urea and 3−5.5 M urea, was in agreement with an intrinsic fluorescence study of HSA conducted at a slightly higher (280 nm) excitation wavelength.[18] Uniquely, the presented method has the capability of measuring structural changes related to both local and global changes in a single measurement.

Loss of HSA's Binding Affinity to Fluorescein As Determined by FIDA. The interaction between HSA and fluorescein was investigated in buffer containing 0−4 M urea using FIDA, and the resulting binding isotherms are shown in Figure 3. The hydrodynamic radius of unbound fluorescein was determined to 0.6 nm. In neat buffer (0 M urea), increasing HSA concentration led to an increase in the apparent hydrodynamic radius of fluorescein from 0.6 to 3.2 nm, thus demonstrating binding of HSA to fluorescein. The data points were fitted to the binding isotherm using eq 3, and the dissociation constant (K_d) and hydrodynamic radius of the

DOI: 10.1021/acs.analchem.9b00537
Anal. Chem. 2019, 91, 4975−4979

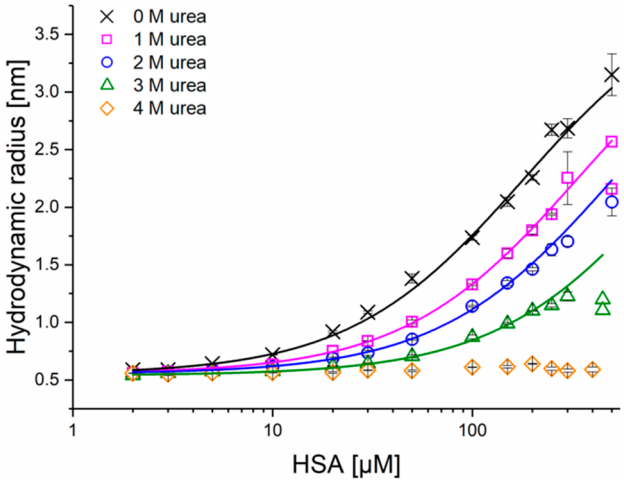

Figure 3. Binding isotherms for the interaction between fluorescein and HSA in phosphate buffer with and without urea at 25 °C. Apparent hydrodynamic radius of fluorescein (10 nM) as a function of HSA concentration; 0 M urea (black crosses), 1 M urea (pink squares), 2 M urea (blue circles), 3 M urea (green triangles), and 4 M urea (orange diamonds) determined by FIDA (n = 3; error bars represent standard deviation, excluding 20 μM, 500 μM at 1 M urea and 450 μM at 3 M urea where n = 2). The solid lines represent individual fitting of the data points to the binding isotherm (eq 3).

complex were determined to be 25.1 μM and 3.93 nm, respectively. These results were as expected, since the complex size was consistent with the determination of HSA in Figure 2A, and the K_d value was comparable to the previously reported value of 35.7 μM.[12]

In Figure 3, it is visually observed that the binding affinity between fluorescein and HSA decreased with increasing urea concentration (1−3 M), and hereafter completely lost at 4 M urea. The data points obtained in 1−3 M urea were fitted to the binding isotherm (eq 3) with the hydrodynamic radius of the complex fixed to the value determined in neat phosphate buffer (3.93 nm). This approach was applied because the data points for 1−3 M urea were obtained in the lower part of the dynamic range, and hence, this served to attain the curve profile plateau at full binding. This assumption was confirmed by the measured HSA sizes in Figure 2A.

Dissociation constants for the binding of HSA to fluorescein at 0−3 M urea concentrations were subsequently obtained from the binding isotherms using eq 3. The K_d values increased with increasing urea concentrations (Table 1) as expected.

Interestingly, the decline in binding affinity was measurable at 1 M urea, i.e. at a urea concentration where changes in both intrinsic fluorescence intensity and hydrodynamic radius of HSA were not detected (Figure 2).

Urea-Induced Denaturation and Unfolding Mechanism of HSA. The presented multitiered approach was capable of a detailed characterization of the denaturation and unfolding process of HSA as induced by urea. At low concentrations of urea (1 M) a substantial decrease in HSA's binding affinity to fluorescein was observed (Figure 3), indicating that the binding site (domain IIA) was undergoing locally structural changes, whereas the intrinsic fluorescence intensity and hydrodynamic radius of HSA were not affected yet. At a slightly higher urea concentration (1.5 M), the intrinsic fluorescence intensity was observed to decrease (Figure 2B) thereby demonstrating local changes near the tryptophan and tyrosine residues in HSA. Finally, at high urea concentration (>4 M), the HSA hydrodynamic radius increased significantly (Figure 2A) thus showing global unfolding, while the binding affinity to fluorescein was totally lost showing loss of functionality in domain IIa.

Overall, the data presented above are in good agreement with previously reported studies on chemically induced unfolding of HSA,[17,18] in which initial unfolding of domain I (having only a modest influence on hydrodynamic radius) is followed by an opening of the tertiary structure of domain II (3−5 M urea) with a substantial change in hydrodynamic radius. Nevertheless, a minor discrepancy was identified since fluorescein has been identified as a ligand to domain IIA,[14] and the functionality of this domain should not be affected until higher urea concentrations (>5 M) as measured by chloroform's binding to domain IIA.[18] The FIDA measurements therefore suggest that fluorescein may binds to another domain of HSA or that the binding site (domain IIA) is affected at relatively low urea concentrations (1 M).

Table 1. Dissociation Constants (K_d) Obtained for the Binding of HSA to Fluorescein at Varying Urea Concentrations at pH 7.4 and 25 °C

urea [M]	K_d [μM]	R^2 for binding isotherm fit
0	25.1	0.99
1	47.1	0.99
2	71.1	0.99
3	139	0.99

CONCLUSIONS

In general, a combination of different techniques is required for a complete description and understanding of protein stability and function. Such measurements may not be feasible due to lack of material or due to limited access to costly instrumentation. In the present work, we propose for the first time a new multitiered approach, based on TDA and FIDA, using one instrument and combining assessment of both local structural changes (intrinsic fluorescence and loss of binding) with global changes in the overall hydrodynamic size of the protein. The TDA and FIDA methodologies require only a few microliters of protein solution and are thus well suited for applications where limited sample amounts are at hand. Furthermore, the approaches presented are automated thereby enabling screening applications for investigating stability in response to, e.g., pH changes, addition of stabilizers or excipients used in drug formulations. The accuracy on the determination of the hydrodynamic radius is in general 3−5%, which also opens up for application in which more subtle structural changes are in play. We therefore envision applications within biopharmaceutical drug development, and fundamental studies on protein stability, unfolding, and functionality.

ASSOCIATED CONTENT

Supporting Information

The Supporting Information is available free of charge on the ACS Publications website at DOI: 10.1021/acs.analchem.9b00537.

Additional experimental details (PDF)

DOI: 10.1021/acs.analchem.9b00537
Anal. Chem. 2019, 91, 4975−4979

AUTHOR INFORMATION

Corresponding Author

*E-mail: Henrik.jensen@sund.ku.dk.

ORCID

Jesper Østergaard: 0000-0003-3448-4237

Henrik Jensen: 0000-0001-6750-2716

Notes

The authors declare the following competing financial interest(s): H.J. and J.O. have commercial interest in FIDA-Tech ApS. M.E.P. and S.I.G. are employees of FIDA-Tech ApS.

ACKNOWLEDGMENTS

Financial support from the Danish Council for Independent Research, Technology and Production Science (Grant 11-106647) and the Carlsberg foundation (Grant 2013_01_0544) is gratefully acknowledged.

REFERENCES

(1) Filipe, V.; Hawe, A.; Carpenter, J. F.; Jiskoot, W. *TrAC, Trends Anal. Chem.* **2013**, *49*, 118−125.

(2) Maarschalkerweerd, A. v.; Wolbink, G. J.; Stapel, S. O.; Jiskoot, W.; Hawe, A. *Eur. J. Pharm. Biopharm.* **2011**, *78* (2), 213−221.

(3) Zölls, S.; Tantipolphan, R.; Wiggenhorn, M.; Winter, G.; Jiskoot, W.; Friess, W.; Hawe, A. *J. Pharm. Sci.* **2012**, *101*, 914−935.

(4) Philo, J. S. *Curr. Pharm. Biotechnol.* **2009**, *10* (4), 359−372.

(5) Cottet, H.; Biron, J.-P.; Cipelletti, L.; Matmour, R.; Martin, M. *Anal. Chem.* **2010**, *82*, 1793−1802.

(6) Cottet, H.; Biron, J.-P.; Martin, M. *Anal. Chem.* **2007**, *79*, 9066−9073.

(7) Jensen, S. S.; Jensen, H.; Cornett, C.; Møller, E. H.; Østergaard, J. *J. Pharm. Biomed. Anal.* **2014**, *92*, 203−210.

(8) Lavoisier, A.; Schlaeppi, J.-M. *mAbs* **2015**, *7*, 77−83.

(9) Taylor, G. *Proc. R. Soc. London Ser. A* **1954**, *225*, 473−477.

(10) Taylor, G. *Proc. R. Soc. London Ser. A* **1953**, *219*, 186−203.

(11) Jensen, H.; Østergaard, J. *J. Am. Chem. Soc.* **2010**, *132*, 4070−4071.

(12) Poulsen, N. N.; Andersen, N. Z.; Østergaard, J.; Zhuang, G.; Petersen, N.; Jensen, H. *Analyst* **2015**, *140*, 4365−4369.

(13) Poulsen, N. N.; Pedersen, M. E.; Ostergaard, J.; Petersen, N. J.; Nielsen, C. T.; Heegaard, N. H. H.; Jensen, H. *Anal. Chem.* **2016**, *88* (18), 9056−9061.

(14) Abou-Zied, O. K.; Sulaiman, S. A. J. *Dyes Pigm.* **2014**, *110*, 89−96.

(15) Millero, F. J.; Drost-Hansen, W.; Korson, L. *J. Phys. Chem.* **1968**, *72* (6), 2251.

(16) Shiu, Y. J.; Jeng, U. S.; Huang, Y. S.; Lai, Y. H.; Lu, H. F.; Liang, C. T.; Hsu, I. J.; Su, C. H.; Su, C.; Chao, I.; Su, A. C.; Lin, S. H. *Biophys. J.* **2008**, *94* (12), 4828−4836.

(17) Leggio, C.; Galantini, L.; Konarev, P. V.; Pavel, N. V. *J. Phys. Chem. B* **2009**, *113* (37), 12590−12602.

(18) Ahmad, B.; Khan, M. K. A.; Haq, S. K.; Khan, R. H. *Biochem. Biophys. Res. Commun.* **2004**, *314* (1), 166−173.

(19) Chamieh, J.; Merdassi, H.; Rossi, J. C.; Jannin, V.; Demarne, F.; Cottet, H. *Int. J. Pharm.* **2018**, *537* (1−2), 94−101.

(20) Peters, T. *All about Albumin*; Elsevier: New York, 1995; p 432.

(21) Santra, M. K.; Banerjee, A.; Rahaman, O.; Panda, D. *Int. J. Biol. Macromol.* **2005**, *37* (4), 200−204.

(22) Østergaard, J.; Jensen, H. *Anal. Chem.* **2009**, *81*, 8644−8648.

DOI: 10.1021/acs.analchem.9b00537
Anal. Chem. 2019, 91, 4975−4979